



UNIVERSITEIT•STELLENBOSCH•UNIVERSITY
jou kennisvennoot • your knowledge partner

E344 Assignment 6

Stéphan van Biljon
22534865

Report submitted in partial fulfilment of the requirements of the module
Design (E) 344 for the degree Baccalaureus in Engineering in the Department of Electrical
and Electronic Engineering at Stellenbosch University.

October 3, 2021



UNIVERSITEIT•STELLENBOSCH•UNIVERSITY
jou kennisvennoot • your knowledge partner

Plagiaatverklaring / *Plagiarism Declaration*

1. Plagiaat is die oorneem en gebruik van die idees, materiaal en ander intellektuele eiendom van ander persone asof dit jou eie werk is.

Plagiarism is the use of ideas, material and other intellectual property of another's work and to present is as my own.

2. Ek erken dat die pleeg van plagiaat 'n strafbare oortreding is aangesien dit 'n vorm van diefstal is.

I agree that plagiarism is a punishable offence because it constitutes theft.

3. Ek verstaan ook dat direkte vertalings plagiaat is.

I also understand that direct translations are plagiarism.

4. Dienooreenkomsdig is alle aanhalings en bydraes vanuit enige bron (ingesluit die internet) volledig verwys (erken). Ek erken dat die woordelikse aanhaal van teks sonder aanhalingstekens (selfs al word die bron volledig erken) plagiaat is.

Accordingly all quotations and contributions from any source whatsoever (including the internet) have been cited fully. I understand that the reproduction of text without quotation marks (even when the source is cited) is plagiarism

5. Ek verklaar dat die werk in hierdie skryfstuk vervat, behalwe waar anders aangedui, my eie oorspronklike werk is en dat ek dit nie vantevore in die geheel of gedeeltelik ingehandig het vir bepunting in hierdie module/werkstuk of 'n ander module/werkstuk nie.

I declare that the work contained in this assignment, except where otherwise stated, is my original work and that I have not previously (in its entirety or in part) submitted it for grading in this module/assignment or another module/assignment.

22534865	S. van Biljon
Studentenommer / Student number	Handtekening / Signature
Voorletters en van / Initials and surname	Datum / Date

Contents

Declaration	i
List of Figures	iii
List of Tables	iv
Nomenclature	v
1. Literature	1
2. System Design	6
3. Detail Design	8
4. Sub-system Results	19
5. System Results	26
Bibliography	27
A. GitHub Activity Heatmap	30
B. Stuff you want to include	31

List of Figures

1.1.	IV and Power relationship of PV module [1]	2
1.2.	Light intensity dependent IV relationships [2]	2
1.3.	Circuit diagram of a battery with internal resistance and a 100Ω load	3
2.1.	Complete System Block Diagram Overview	6
2.2.	Detail of each Subsystem of the Complete System	7
3.1.	LT317A Regulator Charging Circuit with High-Side Switch	9
3.2.	High-side PMOS switch with NMOS driver	10
3.3.	Operational Amplifier Under-voltage Protection Circuit with a High-side Switch	13
3.4.	Complete Assignment 4 Circuit Diagram	15
3.5.	Examples of Low-side Switches [3]	15
3.6.	Supply Voltage Measurement Circuit	16
3.7.	Battery Voltage Measurement Circuit	18
4.1.	Simulation Output and Values	19
4.2.	Simulation Output and Values	21
4.3.	TSC213 Output Voltage vs Current through R_{SENSE}	22
4.4.	Measured Noise Suppression Results	22
4.5.	Simulated Supply Voltages vs Circuit Output Voltages	24
4.6.	Supply Voltage Measurement Circuit Response Time	24
4.7.	Simulated Battery Voltages vs Circuit Output Voltages	25
4.8.	Battery Voltage Measurement Circuit Response Time	25
5.1.	PCB with barcode and student card	26
B.1.	High-side PMOS switch [4]	31
B.2.	High-side PMOS switch with NPN driver [5]	31
B.3.	Charging stages of a battery [6]	32
B.4.	RS-4AH Discharge Characteristics [7]	32
B.5.	Hysteresis Curve of an Inverting Schmitt Trigger with $V_{REF} = 0V$ [8]	32
B.6.	Current Draw of the 5V Rail (B) with a Voltage Over the Load (A)	33

List of Tables

1.1.	Voltage and current measurements of the SLP005-12 PV module	2
4.1.	Measured Charging Voltage of the Charging Circuit	20
4.2.	Measured Switch Terminal Voltages	20
4.3.	Measured Discharge Threshold Voltages	21
4.4.	Measured TSC213 Output Voltages and I_{SENSE} Current	22
4.5.	Measured Switch Terminal Voltages and Drain Currents	23
4.6.	Measured Supply Voltage vs Measured Output Voltage	24
4.7.	Measured Battery Voltage vs Measured Output Voltage	25

Nomenclature

Variables and functions

V_{OC}	Open-circuit voltage of a PV module/cell.
I_{SC}	Short-circuit current of a PV module/cell.
V_{MP}	Maximum power point voltage.
I_{MP}	Maximum power point current.
V_{SG}	Source-gate voltage of a P-channel MOSFET.
V_{GS}	Gate-source voltage of an N-channel MOSFET.
V_{TP}	Thresh-hold voltage of a P-channel MOSFET.
V_{TN}	Thresh-hold voltage of an N-channel MOSFET.
V_G	Gate voltage of a MOSFET.
V_S	Source voltage of a MOSFET.
V_{DS}	Drain-source voltage of an N-channel MOSFET.
V_{SD}	Source-drain voltage of a P-channel MOSFET.
I_D	Drain current of a MOSFET.
V_F	Forward voltage of a Schottky diode.
T_j	Junction temperature of the LM317T regulator.
T_{amb}	Ambient temperature of the atmosphere.
R_{thJA}	Junction to Ambient thermal resistance.
R_{thJC}	Junction to Case thermal resistance.
R_{thCS}	Case to Sink thermal resistance.
R_{thSA}	Sink to Ambient thermal resistance.
P_D	Power dissipated by the LM317T regulator.
I_{FP}	Peak Forward Diode Current.
V_{DI}	Differential Voltage.
V_{CMR}	Common Mode Voltage.
V_{LT}	Lower Threshhold Voltage of an Op-Amp.
V_{UT}	Upper Threshhold Voltage of an Op-Amp.
V_{BI}	Beetle ADC Input Voltage.
V_{PS}	Power Supply Voltage.

Acronyms and abbreviations

PV	Photo-voltaic.
IV	Current-voltage.
V	Voltage.
A	Ampere.
Ω	Ohm.
Ah	Amp-hour.
Wh	Watt-hour.
C	Measure of the rate at which a battery is discharged relative to its maximum capacity.
MOSFET	Metal–Oxide–Semiconductor Field-Effect Transistor.
PMOS	P-channel MOSFET.
NMOS	N-channel MOSFET.
BJT	Bipolar Junction Transistor.
DC	Direct Current.
AC	Alternating Current.
LED	Light Emitting Diode.
RC	Resistor and capacitor filter time constant.
ADC	Analogue to Digital Conversion.

Chapter 1

Literature

Solar Photovoltaic Cells and Solar Modules

A solar, photo-voltaic cell is a device, within which, the electrical characteristics vary when exposed to different levels of light. A PV cell absorbs the energy of photons and through the photovoltaic effect, creates a potential difference and induces the flow of current. This flow of current is created by the PV cell in order to be extracted through conductive metal contacts and to be used as an energy source [9].

Although PV cells and modules are used as a energy source, due to the fact that our PV modules are made of multi-crystal silicon (which allows less freedom for the electrons to move), the efficiency of solar energy to usable energy conversion is only in the range of 13-16% [10].

Two important electrical characteristics of PV modules (illustrated in Figure 1.1) includes the open circuit voltage and the short circuit current. The open circuit voltage of a solar PV module is the sum of the open circuit voltages created by each PV cell, which is the maximum voltage available from a PV cell, when the current through each cell is at a minimum (0A) [11]. The short circuit current of a solar PV module is the maximum current available from a PV module, when the voltage through each cell is at a minimum (0V) [12].

Polycrystalline PV cells typically have a V_{OC} of 0.6V [11] and since the SLP005-12 PV module has 36 cells, the calculated V_{OC} of 21.6V matches the datasheet value given [13]. The short circuit current of the PV module is listed as 0.34A [13].

Another important characteristic of PV modules is the maximum power point. As seen in Figure 1.1, which shows the IV relationship within a PV module, the maximum power point is the operating voltage and current, V_{MP} and I_{MP} , where the PV module gives the maximum power output [1]. The rated power that the SLP005-12 PV module can output is 5W [13].

When the values listed on the datasheet of the SLP005-12 PV module are tested for, they are tested for under Standard Test Conditions [14]. These conditions require:

- Solar radiation (light intensity) of $1 \frac{kW}{m^2}$. This is the average energy of the sun at sea level.
- Cell temperature of 25°C.
- Air Mass = 1.5 and no wind

The current-voltage relationship in a PV module will change under non-standard test conditions. For example, Figure 1.2 shows how the curve shifts upwards for increasing light intensity. When measuring the SLP005-12 open circuit voltage and short circuit current, this changing relationship was encountered during different light intensities shown in Table 1.1. The large variance of the measured current contrasted with the small variance of the measured voltage is confirmed by the light intensity dependant IV relationship from Figure 1.2.

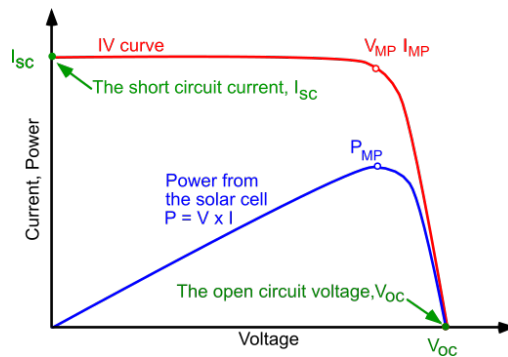


Figure 1.1: IV and Power relationship of PV module [1]

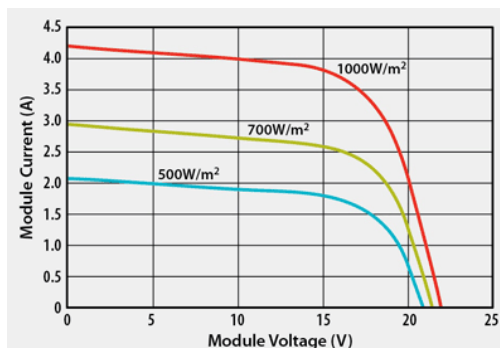


Figure 1.2: Light intensity dependent IV relationships [2]

Table 1.1: Voltage and current measurements of the SLP005-12 PV module

	V_{OC} [V]	I_{SC} [A]
Theroretical per cell	0.6	0.094
Datasheet per module	21.6	0.34
Measured Ambient Light	11.71	0.24
Measured Dark (covered)	0	0
Measured Upside-down (sun)	15.55	0.46
Measured Oblique (sun)	19.87	0.6
Measured Perpendicular (sun)	21.6	0.66

Lead Acid Batteries

Lead acid batteries are the most commonly used type of rechargeable battery in photo-voltaic systems due to their long lifetime and low costs. [15]. The measured open circuit voltage of the RS-4AH battery is 6.37V. This stands in contrast to the 6V nominal rating of the battery (2V per cell for 3 cells) [7]. Nominal values are approximate values that are used to classify different batteries and so measured values are the most accurate.

The advertised battery capacity is 4Ah (or 24Wh) [7] which means that if you use the battery to supply 4A of current for an hour, the battery will be depleted. Ah is a useful measurement value due to the fact that a battery is a time-variable current supply for loads in circuits. This advertised capacity is not accurate when discussing the actual, available capacity of the battery. Battery capacity is dependent on temperature (where higher temperature will increase your battery capacity at the cost of battery life and vice versa [16]) but more importantly, only 10-15% of the advertised capacity can be used to ensure battery longevity [17].

The RS-4AH battery has an internal resistance of approximately $45\text{ m}\Omega$. Internal resistance is the resistance of a battery or cells as opposed to the resistance of a load connected to a power source [18]. This internal resistance of the battery, illustrated in Figure 1.3 is the reason that the voltage across the terminals of the battery will drop if a load is connected [19].

Self discharge is a phenomenon that occurs when chemical reactions inside of a battery reduce the stored charge while not being connected to a load. The RS-4AH battery will self discharge 40% of its capacity at room temperature over 12 months [7].

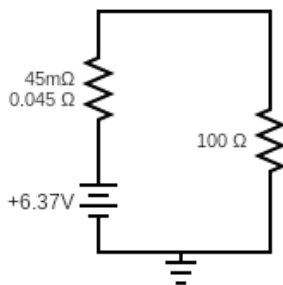


Figure 1.3: Circuit diagram of a battery with internal resistance and a $100\ \Omega$ load

Battery Charging

There are 4 stages when dealing with battery charging , but the 4_{th} stage, Equalization, is optional and is recommended to be done every 3 to 6 months [7]. When a 4Ah battery is fully charged, it draws a current of about 40-80mA [6]. Refer to Figure B.3 when considering the charging stages [6].

- **Bulk Charge Mode** - The depleted battery is being charged with constant current (max of 1.2A [7]) while the battery voltage is allowed to rise linearly. This is where 80% (5.4V) of the battery capacity is returned.
- **Absorption Mode** - When 80% of the battery capacity has been returned, the battery voltage is held constant while the battery current decreases linearly until it reaches 40-80mA. This is the stage where the last 20% (1.35V) of the battery capacity is returned.
- **Float Mode** - When the battery current reduces to 40-80mA, the battery voltage is maintained at 2.25V per cell or 6.75V for a nominal 6V lead-acid battery. This is the voltage of a fully charged battery.
- **Equalization Mode** - This is an optional charging stage that is used to remove the build-up of negative chemical reactions by overcharging the battery with a very small current for a few hours.

Battery Discharging

The RS-4AH battery can discharge at a rate of up to 60A [7]. If we apply a 100Ω load as shown in Figure 1.3, the 100Ω load (250mW rating) will heat up to the point of melting because the power dissipated is almost double its rating!

The RS-4AH battery is considered to be fully depleted when each cell is at a voltage of 2V [7] ($\therefore 6V$ for the battery). Only using 10-15% of the advertised capacity will ensure the longevity of this non-deep cycle, lead-acid battery [17].

Depending on the rate at which you discharge the battery, the terminal voltage of the battery will decrease at different rates. This is to say, although a current of $0.05C$ where C is 4Ah is 20 times smaller than $1C$, the terminal voltage of the battery will not decrease 20 times slower when comparing the rate of discharge.

Refer to Figure B.4. For example, a current of $0.05C$ drawn for 60 minutes will not have a noticeable terminal voltage decrease [7] while a current of $1C$ drawn for 22 minutes will completely deplete the battery [7]. If we extrapolate this, we will find that a current draw of $0.05C$ will not completely deplete the battery in 20 times more time (7.33 hours). A discharge rate of 200mA used for 20 hours will fully deplete the battery and it will take 11 hours for the voltage of each cell to reach 2V [7].

Fuses

The purpose of a fuse is to protect circuitry when a fault in a load or a part of the circuit causes too much current to flow, thus damaging components. The time-current characteristics of a fuse determine how quickly it will respond to overcurrents. All fuses have inverse time-current characteristics. The greater the overcurrent, the quicker the fuse will blow [20].

The current carrying capacity of a fuse is also dependent on its ambient temperature. Higher temperatures allow the fuse to respond faster to overcurrents while lower temperatures make the response to overcurrents slower [20]. When a fuse experiences an overcurrent, it will naturally increase in temperature and melt to protect the circuitry. The shelf-life of a typical fuse is a few decades since they are made out of copper or silver which does not retain moisture easily, however, fuses may trip at a lower current after excessive use or time [21].

Chapter 2

System Design

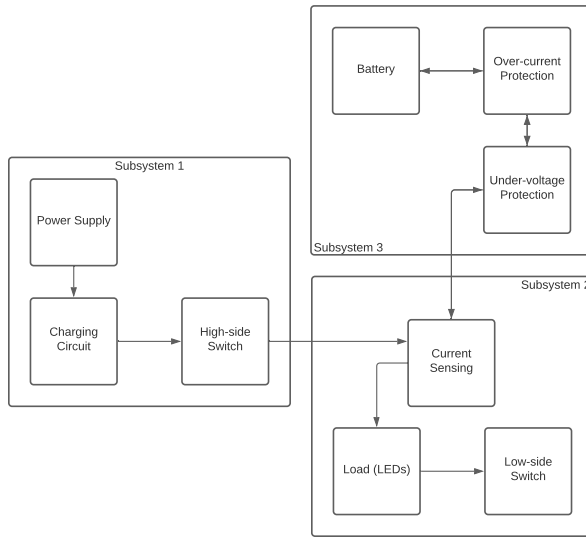


Figure 2.1: Complete System Block Diagram Overview

The complete system overview can be considered according to Figure 2.1 above. For Subsystem 1 which is represented in Figure 2.2a: The system consists of a DC power supply unit connected to a charging circuit (which is connected through a high-side switch) to a load.

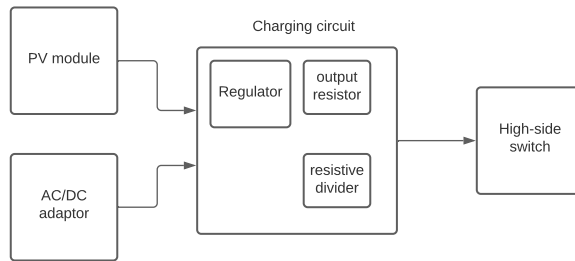
A SLP005-12 PV module or a 12V DC/AC can be used as the input for the charging circuit. The circuit consists of a LM317T regulator which has been chosen for its ability to produce an adjustable output voltage (This is a good choice in terms of flexibility). The circuit supporting the regulator has a resistive divider which allows the output voltage to be chosen as well as an output resistor to allow low charging currents for a fully charged RS-4AH battery [22].

The high-side switch connects the charging circuit to a load (which will be the 6V battery, current sensing and under-voltage protection). The switch acts as a way to disconnect the circuit from the battery when it's fully charged as well as connecting the battery to a charger.

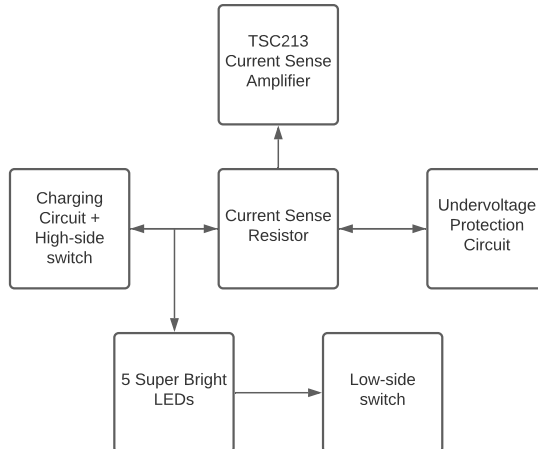
The bi-directional current sensing subsystem seen in Figure 2.2b consists of a current sense amplifier with a current sense resistor (which is connected to the under-voltage protection circuit and the charging circuit), a load of 5 super bright LEDs and a low-side switch . The current sense resistor creates a voltage drop when current is passed through it. This small

voltage drop is amplified by the TSC213 operational amplifier and a corresponding V_{OUT} is created in order to measure the current flowing to/from the battery. The low-side switch connects/disconnects the load to/from ground to control the current through the LEDs.

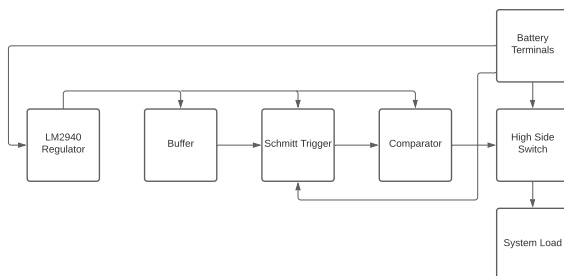
The under-voltage protection system seen in Figure 2.2c consists of a voltage regulator, a buffer, a Schmitt trigger, a comparator and a high-side switch. The regulator powers the components and acts as the basis for a reference voltage. The trigger determines the state of the system based on voltage thresholds and previous states. The comparator inverts the trigger output and the switch controls the discharging of the battery. An LM2940 regulator has been chosen due to the need of a 5V power supply and it's low operating input voltage. Each subsystem works in union to produce the overall system which allows a battery to be charged from a power supply as well as a load to be powered by a battery.



(a) Subsystem 1 Overview



(b) Subsystem 2 Overview



(c) Subsystem 3 Overview

Figure 2.2: Detail of each Subsystem of the Complete System

Chapter 3

Detail Design

Voltage Regulation

Since the LM317T has an adjustable output voltage of 1.2 to 37V, an input voltage range of 3 to 40V [22] is valid. This is because voltage regulators typically need an input voltage that is 2 to 3V higher than the output voltage.

For the charging circuit that was designed, the output voltage of the regulator-switch circuit needed to be equal to 7.2V, which is the equalization charge voltage of the battery [7]. When the battery is fully charged at 7.2V, very little current will flow through the diode attached to the battery terminals which is illustrated in Figure 3.1. This causes V_F to be small ($\approx 0.4V$ [23]). This voltage drop then results in the output of the regulator, $V_O = V_{Battery} + V_F = 7.6V$ since the voltage drop over R_5 and the PMOS V_{SD} is negligible for very small currents [24].

From this desired output voltage, the input voltage to the regulator circuit needs to be at least 10V and higher. For this reason, a 12V AC/DC adaptor and a PV module with a $V_{OC} = 21.6V$ [13] has been chosen as the power supplies to this charging circuit. In order to achieve the desired output voltage of the LM317T, a resistive divider consisting of R_1 and R_2 as seen in Figure 3.1 needs to be implemented. The design equation: $V_O = V_{REF} \left(1 + \frac{R_2}{R_1} \right)$ can be used to determine the value of this resistive divider (which is done in the section below). Typically, $V_{REF} = 1.25V$ for design purposes [22].

Current limit

The LM317T has a maximum and minimum load current that needs to be adhered to: $I_{O(max)} = 0.4A$ and $I_{O(min)} = 3.5mA$ [22] in order for it to operate. This limits how quickly the battery can charge but it is a necessary part of the regulator operation.

Since the current is very small when the battery is fully charged, only the resistive divider path can draw the current necessary to fulfil $I_{O(min)}$. Using the design equation from above and solving simultaneously with: $V_O = I_{O(min)}(R_1 + R_2)$, $R_1 \approx 360\Omega$ and $R_2 \approx 1.8\text{k}\Omega$. The values seen in Figure 3.1 are as a result of resistor tolerances.

Since we know that $V_O = 7.6V$ and that when the battery is depleted (6V), the current drawn will be the largest. This large current, up to $I_{O(max)}$, will cause the diode $V_F = 0.53V$ [23]. This results in the PMOS V_S node = $V_{Battery} + V_F = 6.53V$. From this, V_{R5} and $I_{R5} \approx I_{O(max)}$

can be used to solve for $R_5 = 2.675 \Omega$. R_S was then adjusted within SPICE to find an optimal value of $R_5 = 0.5 \Omega$.

Thermal analysis

The characteristics of the LM317T regulator will change if the temperature of the device is drastically above 25°C . For example, the $I_{O(\max)}$ value used above is rated for 25°C . As T_j rises, the $I_{O(\max)}$ will decrease at different input-output differentials compared to $T_j = 25^\circ \text{C}$ [22]. The reference voltage, V_{REF} , will also decrease at higher junction temperatures [22].

The maximum power dissipated within the LM317T can be calculated as: $P_{D(\max)} = V_{Regulator} \times I_{O(\max)}$. We know that $I_{O(\max)} = 0.4\text{A}$ and $V_{Regulator} = V_I - V_O$. $V_O = 7.6\text{V}$ as calculated above and $V_I = V_{Supply} - V_F$ when $I_{input} = I_{O(\max)}$. $\therefore V_F = 0.53\text{V}$ [23], $V_I = 11.47\text{V}$ and $V_{Regulator} = 3.87\text{V}$. This results in the regulator $P_{D(\max)} = 1.548\text{W}$ which is within the limits of the LM317T power dissipation of 20W [22].

Assuming that no heat-sink is present: $P_D = \frac{T_j - T_{amb}}{R_{thJA}}$ where $R_{thJA} = 50^\circ \text{C/W}$ [22] and $T_{amb} = 25^\circ \text{C}$. From this, we can conclude that $T_j = 102.4^\circ \text{C}$. This temperature will affect the regulator characteristics and needs to be decreased with a heat-sink. Now assuming the addition of a heat-sink: For the TO-220 5772 heat-sink, when $P_D = 1.548\text{W}$, $R_{thSA} = 7.8^\circ \text{C/W}$ [25]. For a TO-220 package tightened with thermal grease, $R_{thCS} = 1^\circ \text{C/W}$ [26]. Finally, for the LM317T regulator, $R_{thCS} = 5^\circ \text{C/W}$ [22]. All of this combines to form the equation: $P_D = \frac{T_j - T_{amb}}{R_{thJC} + R_{thCS} + R_{thSA}}$ where you can solve for $T_j = 46.36^\circ \text{C}$.

Not only has the addition of the heat-sink improved the performance of the regulator, in terms of higher output currents and reference voltages, but it has also made the casing of the LM317T regulator safe to touch. This was all done by reducing T_j of the regulator.

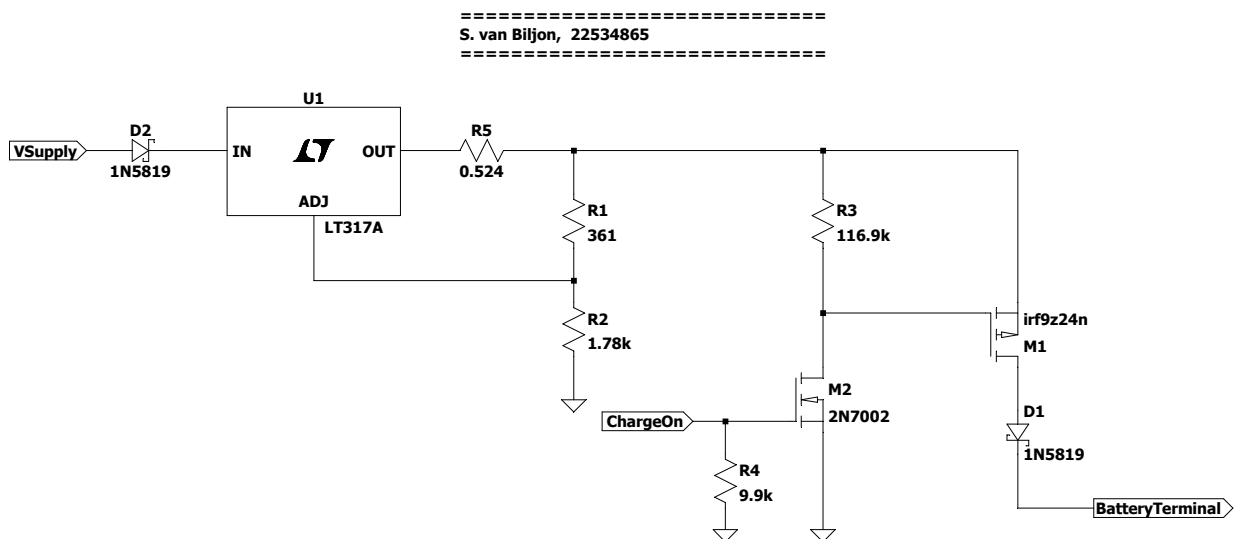


Figure 3.1: LT317A Regulator Charging Circuit with High-Side Switch

High-side Switch on Supply Side

A high-side switch was designed to connect a charging circuit to a load (a battery). MOSFETs are more applicable to large current applications compared to BJTs [27] and the IRF9Z24NPbF PMOS can handle a drain current of up to 12A [24]. A DC supply is chosen to charge the load (battery) because an AC supply will change polarities, thus charging and then discharging a load.

Current must not flow back into the charging circuit or supply from the load. A diode only allows current to flow in one direction and so a Schottky diode has been used due to its applications for renewable energy. [28]. Refer to Figure 3.2 when considering the design calculations below.

A 5V control signal results in the NMOS $V_{GS} = 5V$ and $V_{TN} = 0.8$ to $3V$ [29] therefore $V_{GS} > V_{TN}$. This turns the NMOS on and pulls V_G of the PMOS to 0V since the NMOS V_{DS} is negligible for very small currents [29]. For the PMOS: $V_S = V_{Battery} + V_F$ where $V_F = 0.45$ to $0.6V$ [23]. The battery terminal voltage is required to be 6 to 7.2V. This results in the PMOS $V_S = 6.45$ to $7.8V$ and the $V_{SG} = V_S$ while $|V_{TP}| = 2$ to $4V$ [24]. The PMOS $V_{SG} > |V_{TP}|$ therefore the PMOS switch is on and current flows from the circuit to the load.

The resistor value, R_3 , can be calculated from the 5V control signal situation. Ideally, very little current should be present as the drain current of the NMOS. The reason for this is that current from the charging circuit which does not flow to the battery is wasted current which causes more power dissipation in the regulator. therefore R_3 has been chosen as a large value of $116.9\text{ k}\Omega$. This value originates from the tolerance of a $100\text{ k}\Omega$ resistor. R_4 is a pull-down resistor that removes the charge from the NMOS V_G when a 0V control is placed after a 5V control. This value can be chosen in the range of about $1\text{-}10\text{ k}\Omega$ for practical purposes.

A 0V control signal results in the NMOS $V_{GS} = 0V$ therefore $V_{GS} < V_{TN}$ and the NMOS is off. The PMOS $V_G = 7.65$ to $7.8V$ due to no current through R_3 and the PMOS $V_{SG} = 0V$. We can see that $V_{SG} < |V_{TP}|$, therefore the PMOS is off and current won't flow to the battery.

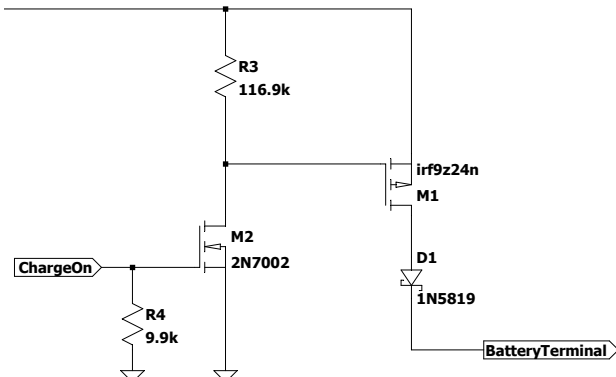


Figure 3.2: High-side PMOS switch with NMOS driver

Over-current Protection

Since the fuse needs to protect from overcurrents, it is helpful to know the current that the battery will typically discharge. The proposed load for the overall system design will be five super-bright LEDs which can each have a peak forward current, $I_{FP} = 100 \text{ mA}$ [30]. Assuming that there will also be a micro-controller drawing current as well as an LED display and a light sensor, it is reasonable to assume that approximately 600mA will be drawn at most. The battery charging current of 400mA can also flow through the switch and in addition to the maximum load current, a fuse of 1A limit should be used.

A fault such as an accidental grounding or a component overload could cause the load current to increase rapidly and since a fuse with a 1A rating will prevent such an overcurrent quickly, it is a good design choice. The 1A fuse has a voltage rating of 32VDC which means that it can safely interrupt a 1A current until 32VDC [31]. That particular voltage level is higher than any individual voltage in the circuit and so it is a safe design. Even if the fuse is used in ambient temperatures lower than room temperature (which will decrease the overcurrents it will blow at), there is enough overhead to stop any faults without impacting on the maximum current draw from the battery, by the load.

Under-voltage Protection

5V rail

The regulator which has been chosen to supply power to the operational amplifiers and to act as a basis for the reference voltage is the LM2940 regulator. It was chosen because it has a lower input voltage of 6V minimum [32] while the LM7805 needs at least 7V [33]. The battery voltage will be the input voltage of the regulator and since the battery will discharge lower than 7V, the LM7805 would not be a suitable choice. The LM2940 will have a typical output voltage of 5V which is suitable for the operational amplifier and high-side switch to function.

High-side switch

A high-side switch was designed to connect the battery terminals to a load/charging circuit. A 5V comparator output results in the NMOS $V_{GS} = 5V$ and $V_{TN} = 0.8 \text{ to } 3V$ [29], therefore $V_{GS} > V_{TN}$. This turns the NMOS on and pulls V_G of the PMOS to 0V since the NMOS V_{DS} is negligible for very small currents [29]. For the PMOS: since the battery terminal voltage $\geq 6V$, this results in the PMOS $V_S \geq 6V$ and the $V_{SG} = V_S$ while $|V_{TP}| = 2 \text{ to } 4V$ [24]. The PMOS $V_{SG} > |V_{TP}|$, therefore the PMOS switch is on and current flows from the battery to the load.

The resistor value, R_8 , can be calculated from the 5V control signal situation. Ideally, very

little current should be present at the drain of the NMOS so that there is little power wastage, therefore $R_8 = 100\text{ k}\Omega$. R_7 is a pull-down resistor that removes the charge from the NMOS V_G when a 0V comparator output occurs. This value is chosen to be $10\text{ k}\Omega$.

A 0V comparator output results in the NMOS $V_{GS} = 0V$, therefore $V_{GS} < V_{TN}$ and the NMOS is off. The PMOS $V_G \geq 6V$ due to no current through R_8 and the PMOS $V_{SG} = 0V$. It can be observed that $V_{SG} < |V_{TP}|$, therefore the PMOS is off and current won't flow from the battery.

Voltage monitoring with hysteresis design

The under-voltage protection circuit contains four stages. The Schmitt trigger, the voltage-follower (buffer), the comparator and the high-side switch. The Schmitt trigger is a comparator with memory. Hysteresis allows the inputs of the trigger to be compared with a reference and then an output is determined based on the previous output of the trigger and threshold voltages. The voltage-follower prevents feedback from influencing the chosen reference voltage. A voltage divider is used so that a custom reference voltage can be selected. A successful design has to respect the limitations of the operational amplifiers. There are 5 limitations for the MCP6421 operating at a $V_{DD} = 5V$ and $V_{SS} = 0V$ [34]:

- Output voltage: $-0.02V \leq V_O \leq 4.98V$ for $I_O \approx 0.5mA$.
- Differential voltage: $V_{DI} \leq 5V$.
- Common mode voltage: $-0.3V \leq V_{CMR} \leq 5.3V$.
- Input voltage: $-1V \leq V_{IN} \leq 6V$.
- Output current: $I_O = \pm 30mA$.

Refer to Figure 3.3 below during the design. We start with the battery resistive divider. From hysteresis, the positive input of the Schmitt trigger, V_{IN2+} , will be the upper threshold voltage (V_{UT} - when the output is high) and lower threshold voltage (V_{LT} - when the output is low) which will change the output of the trigger. Voltage division leads to an expression:

$$\frac{R_4}{R_3 + R_4}(V_{battery}) = V_{IN2+}$$

where $V_{battery} = 6V$ when $V_{IN2+} = V_{LT}$ and $V_{battery} = 6.2V$ when $V_{IN2+} = V_{UT}$. Choosing $R_3 = R_4 = 150\text{ k}\Omega$ gives $V_{LT} = 3V$ and $V_{UT} = 3.1V$. Doing nodal analysis at the positive input of the Schmitt trigger, V_{IN2+} , will give us an equation for V_{LT} and V_{UT} of the hysteresis curve (which we have values for). The Schmitt trigger resistors can then be solved. The nodal analysis of V_{IN2+} leads to the equation:

$$V_{IN2+} = (V_{O1})\frac{R_6}{R_5 + R_6} + (V_{O2})\frac{R_5}{R_5 + R_6}$$

where $V_S = (V_{O1}) \frac{R_6}{R_5 + R_6}$ is the shift of a typical hysteresis curve shown in Figure B.5. The hysteresis dead band needs to be 0.1V since $V_{UT} - V_{LT} = 0.1V$. This difference represents a physical 0.2V change in the battery voltage from 6V to 6.2V. Since V_{UT} and V_{LT} is simply V_{IN2+} evaluated at high and low outputs of the Schmitt trigger, we can conclude that $V_{IN2+(high)} - V_{IN2+(low)} = 0.1V \therefore$

$$\frac{V_{O1}R_6 + V_{O2(high)}R_5}{R_5 + R_6} - \left(\frac{V_{O1}R_6 + V_{O2(low)}R_5}{R_5 + R_6} \right) = 0.1V$$

From this equation, $R_5 = 1\text{k}\Omega$ and $R_6 = 49\text{k}\Omega$ when $V_{O2(high)} \approx 5V$ and $V_{O2(low)} \approx 0V$. The hysteresis curve needs to be shifted such that the origin is now in the middle of V_{LT} and V_{UT} , $\therefore V_S = 3.05V$. From this, $(V_{O1}) \frac{R_6}{R_5 + R_6} = 3.05$ and $V_{O1} = 3.112V$. V_{O1} is the output of the voltage-follower where $V_{O1} = V_{IN1+}$. Through resistive division, we can find that:

$$\frac{R_2}{R_1 + R_2}(5V) = V_{O1}$$

where $R_1 = 34\text{k}\Omega$ and $R_2 = 56\text{k}\Omega$. The comparator takes in the output of the Schmitt trigger as the input to it's negative terminal. This output is then compared to the positive terminal of the comparator ($V_{IN3+} = V_{O1}$). The comparator then flips the output to the rail voltage of 5V or 0V based on this comparison. Every input of the operational amplifiers respect the common mode voltage, differential voltage and maximum input voltage limitations.

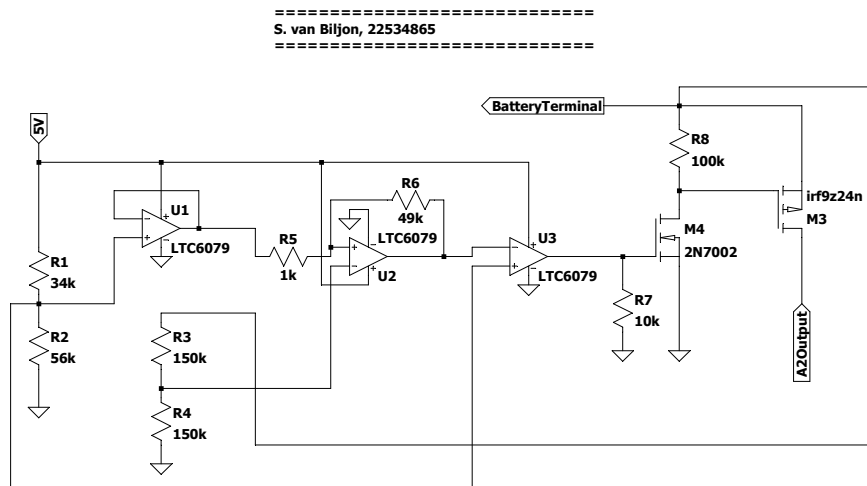


Figure 3.3: Operational Amplifier Under-voltage Protection Circuit with a High-side Switch

Current Sense

The bi-directional current sensor needs to represent the current flowing through the current sensing resistor to or from the battery. For this objective, currents from -150mA (discharging) to 450mA (charging) need to be represented as an analogue output voltage by the TSC213. This results in a current range of 600mA that needs to be represented on a voltage range of 5V (0V to $V_{CC} = 5V$) [35]. When current flows through the 0.1Ω current sensing resistor, the shunt voltage range is from -0.015V to 0.045V (assuming positive current is charging current). This voltage range is then amplified and represented on V_{OUT} by the TSC213 according to the following equation where the gain is fixed at $50\frac{V}{A}$ [35]:

$$V_{OUT} = (R_{SENSE} \times I_{SENSE}) \times Gain + V_{REF}$$

For optimal output voltage swing, you will want your voltage range (0V to $V_{CC} = 5V$) split in half when the current range (600mA) is also split in half. This correlates to $I_{SENSE} = 150mA$ when $V_{OUT} = 2.5V$. Using the equation above, the desired $V_{REF} = 1.75V$. This offset is required for optimal output voltage swing when we have an unbalanced input voltage (due to an unbalanced current range). For V_{REF} , it is seen that 450mA correlates to $V_{OUT} = 4V$ and -150mA correlates to $V_{OUT} = 1V$. This provides an output voltage swing of $3V_{pk-pk}$ around 2.5V. In order to provide the appropriate V_{REF} to the TSC213, voltage division from $V_{CC} = 5V$ needs to be done:

$$V_{REF} = \frac{R_2}{R_1 + R_2} \times V_{CC}$$

R_1 is chosen as $150\text{k}\Omega$ to minimize power losses, which results in $R_2 = 80.77\text{k}\Omega$. This V_{REF} then needs to be fed through a voltage-follower in order to ensure that the TSC213 samples the correct voltage. The final step in designing the bi-directional current sensing circuit is creating a filter to attenuate frequencies above 50Hz such that $1mV_{pk}$ noise on the 5V supply rail and $1mV_{pk}$ noise on R_{SENSE} results in less than $2mV_{pk}$ noise on V_{OUT} . This can be done using a passive, RC filter attached to the output of the TSC213. Since we want to attenuate frequencies above 50Hz, we can use the low-pass filter design equation:

$$f_c = \frac{1}{2\pi RC}$$

Where RC is the desired time constant of the filter and $f_c = 50\text{Hz}$. A higher capacitance will result in more filtering of V_{OUT} but it will also slow down the system. In order to keep the system responsive to current changes (a current change will result in the correct V_{OUT} within 2s), the capacitance was chosen as $C = 4.7\mu F$. This resulted in $R = 677\Omega$.

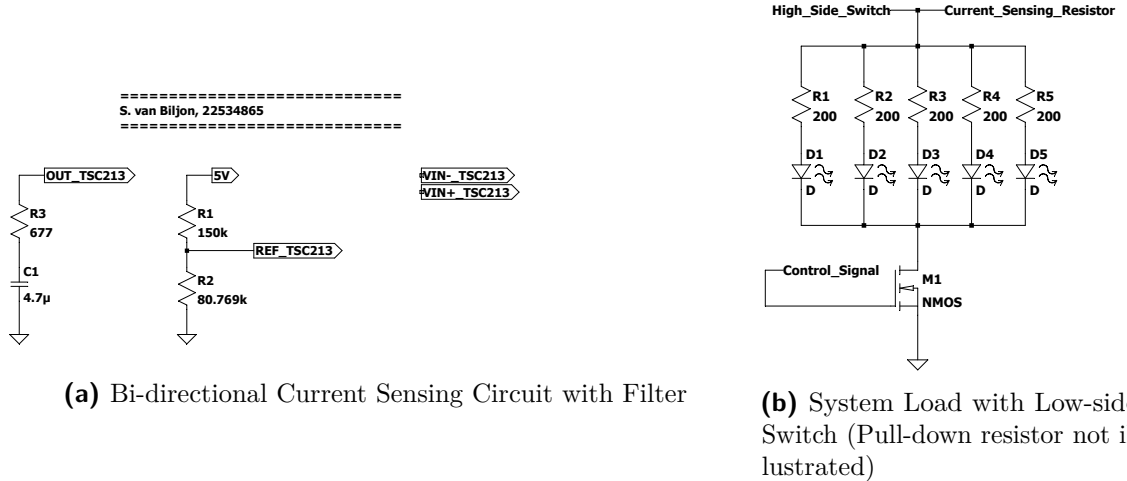


Figure 3.4: Complete Assignment 4 Circuit Diagram

Low-side Switch

A low-side switch was designed to connect/disconnect the system load (5 super bright LEDs) to/from ground. When the switch is on, the load will be grounded and current can discharge into the load, from the battery. A 5V control signal results in the NMOS $V_{GS} = 5V$ and since $V_{TN} = 0.8$ to $3V$ [29], we find that $V_{GS} > V_{TN}$. This turns the NMOS on and connects the load to ground since the NMOS V_{DS} is negligible for very small currents.

The load is designed to draw 100mA of current for a fully charged battery which will make the NMOS drain current: $I_D = 100mA$. In order to limit the load current to 100mA, each LED has to draw 20mA of current. This can be done by placing a 200Ω resistor in series with each LED. $I_D = 100mA$ will not exceed the maximum drain current of the NMOS 2N7000 which is 200mA [29]. For 100mA of drain current and a $V_{GS} = 5V$, $V_{DS} \approx 0.1V$ which can be assumed to be negligible [29].

For a control signal of 0V, $V_{GS} = 0V$ and so $V_{GS} < V_{TN}$. This turns the NMOS off and disconnects the load from ground, thus preventing current flow through the load. Since a MOSFET will act as a voltage controlled switch, it requires very small amounts of current to work but it can also sink the maximum current that the load is designed to draw.

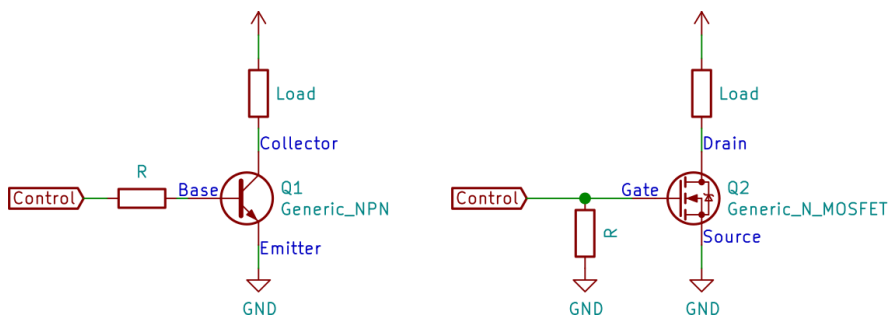


Figure 3.5: Examples of Low-side Switches [3]

Supply Voltage Measurement

A supply voltage measurement circuit was designed to measure the supply voltage and output a signal that is proportional to the measured voltage. The full range of supply voltages (0V to 22V for the PV module) needs to be represented on a 0V to 5V scale. This 0V to 5V output signal of the circuit is compliant with the voltage range limitations of the Beetle's analogue ADC input [36] and ensures the maximum resolution for voltage measurement.

In order for the supply voltage to be represented on a 0V to 5V scale, the output of the circuit must be 0V when the supply voltage is 0V whilst being 5V when the supply voltage is 22V. A voltage divider, as shown in Figure 3.6, can be implemented to satisfy the conditions above. Choose $R_1 = 330\text{ k}\Omega$ in order to minimize current wastage and power losses. R_2 can then be solved for:

$$V_{BI} = \frac{R_2}{R_1 + R_2}(V_{PS})$$

If $V_{BI} = 5V$ and $V_{PS} = 22V$, $R_2 = 97\text{ k}\Omega \approx 100\text{ k}\Omega$. The circuit output will be fed into the ADC input of the Beetle micro-controller, which means that noise needs to be limited in order to ensure an accurate voltage measurement. For this purpose, capacitor C_1 filters out high frequency noise which originates from the AC/DC adapter. Due to the quantization error and the 10 bit resolution of the Beetle [36], the smallest change in the ADC output (one LSB) corresponds to:

$$\frac{V_{REF+} - V_{REF-}}{2^N - 1} = \frac{5 - 0}{2^{10} - 1} = 4.89mV$$

The noise should therefore be suppressed to less than $4.89mV_{PK-PK}$ in order to always represent the correct voltage on the ADC output. The value of C_1 was chosen as 100nF in order to sufficiently suppress the noise without making the circuit response time more than 100ms for a 1V step change.

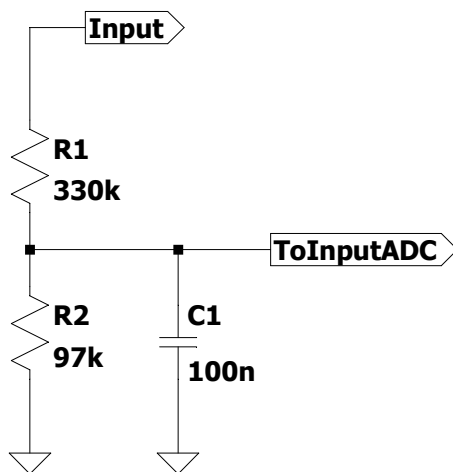


Figure 3.6: Supply Voltage Measurement Circuit

Battery Voltage Measurement

A battery voltage measurement circuit was designed to measure the battery voltage and output a signal that is proportional to the measured voltage. The full range of realistic battery voltages (5.5V to 7.5V) also needs to be ideally represented on a 0V to 5V scale. This voltage range is, however, limited by the output of the MCP op-amp: $35mV \leq V_O \leq 4.965V$ [34]. After taking this limitation into account, as well as adding a safety margin to account for possible clipping of the op-amp output due to resistor tolerances, a range of 0.1V to 4.9V will be output by the circuit and fed into the Beetle's analogue ADC input.

An op-amp will be used as a differential amplifier that can "zoom" in on the battery voltage range. The 2V battery voltage range will be represented on a 0.1V to 4.9V range. This provides a higher resolution than a voltage divider which would represent 0V to 7.5V on the chosen range, thus wasting 73% of the range since the battery should never deplete below 5.5V (If we take a safety margin into account).

An analysis of the differential amplifier (shown in Figure 3.7 as U2) can be done in order to find values for R_5 , R_6 , R_7 and R_8 . If a node analysis is done at V_- of U2, an expression for the differential amplifier can be found as:

$$V_{REF} = V_- \left(\frac{R_5 + R_6}{R_5} \right) - V_{OUT} \left(\frac{R_6}{R_5} \right)$$

If we choose $R_7 = R_8 = 100\text{k}\Omega$ (less current and power wastage), then $V_+ = \frac{V_{BAT}}{2} = V_- = 2.75V$ to $3.75V$. The battery voltage range is $V_{OUT} = 0.1V$ to $4.9V$. Using the minimum and maximum values of V_- and V_{OUT} above, R_5 and R_6 can be simultaneously solved for as:

$$\frac{R_5}{R_6} = 3.8$$

Choosing $R_5 = 68\text{k}\Omega$, we find that $R_6 = 17.89\text{k}\Omega \approx 18\text{k}\Omega$. We can now solve for V_{REF} using the formula above, to find $V_{REF} = 3.447V$. This V_{REF} will be created from the regulator 5V output using resistive voltage division, as seen in Figure 3.7:

$$V_{REF} = \frac{R_3}{R_3 + R_4} (5) \quad (5)$$

Again, in order to minimize current and power wastage, choose $R_4 = 68\text{k}\Omega$ and solve for $R_3 = 151.35\text{k}\Omega \approx 150\text{k}\Omega$. In order to prevent the feedback of the differential amplifier from influencing V_{REF} , a voltage follower is used. The output of the differential amplifier, V_{OUT} , will stay within the ADC input limitations, will have no noise (no AC component affects the battery) and will respond to an input in less than 100ms for a 1V step change.

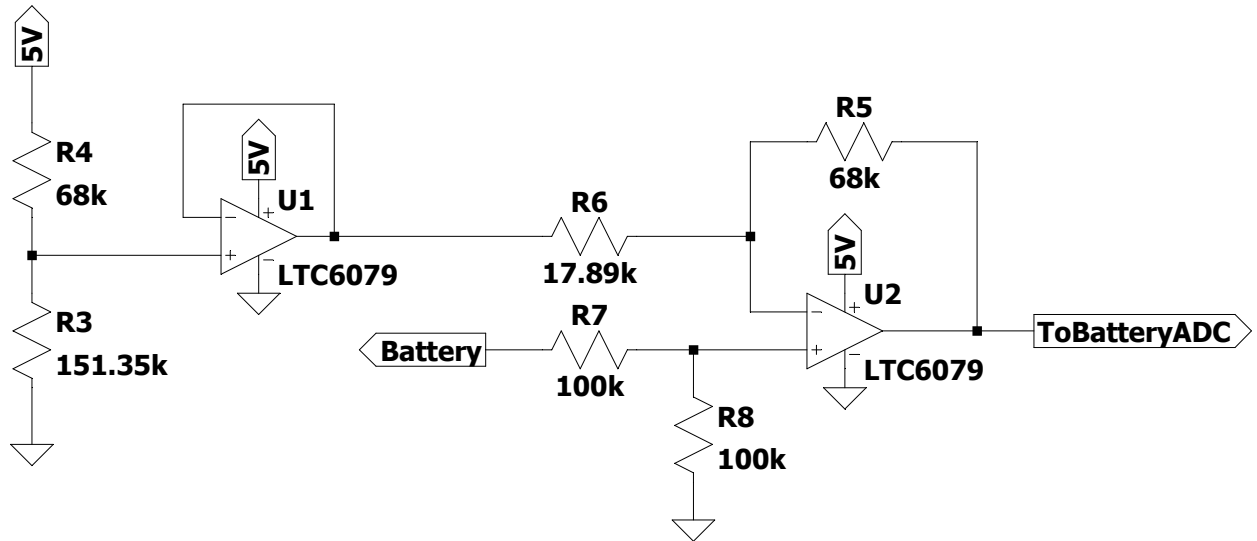


Figure 3.7: Battery Voltage Measurement Circuit

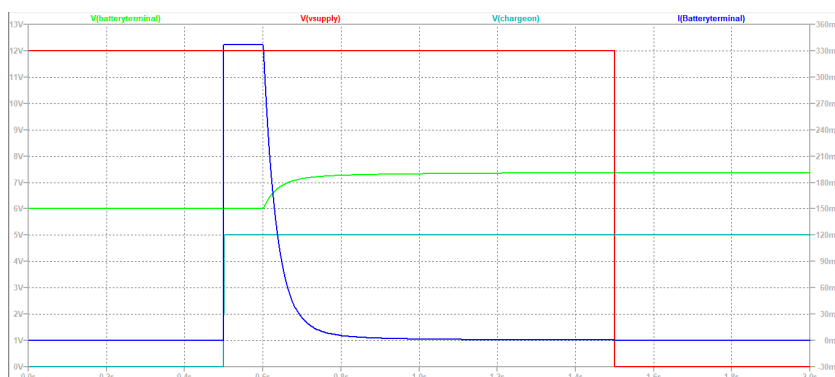
Chapter 4

Sub-system Results

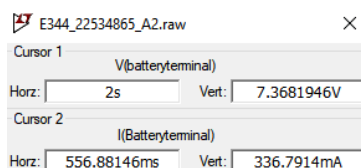
Voltage Regulation

Refer to Figure 4.1 below when taking the simulation results into account. At time = 0, the DC power supply is 12V (high) and the control signal is 0V (low) \therefore the depleted battery level (6V) does not charge. When the control signal goes high at $t = 0.5\text{s}$ while the supply is still high, the depleted battery starts to charge after 0.1s. As seen in Figure 4.1a, the battery level starts to rise while the charging current decreases from a limit of 337mA. 300 to 400mA is the range which can be provided by the PV module power supply.

When the battery becomes fully charged at 7.37V (which is in the range of equalization charge), the current that the battery draws drops close to 0mA. The resistive divider draws enough current to keep the regulator functioning. Due to the placement of Schottky diodes in the circuit, the battery does not discharge when the switch is on and the power supply drops to 0V (low). The power dissipation of the regulator can be calculated as 1.45W. The output voltage of the charging and switch circuit, as well as the current that the battery draws, and the regulator power dissipation are within acceptable ranges \therefore the circuit works as expected.



(a) Simulation Battery Voltage and Current, Supply Voltage and Control Voltage



(b) Simulation Battery Voltage and Current Values

Figure 4.1: Simulation Output and Values

Found in Table 4.1, the charging voltage of the circuit was measured under no load, $1\text{ k}\Omega$ and $10\text{ k}\Omega$ conditions. Under a no load condition, the charging voltage measures higher than the load conditions. The lower the value of load resistance, the more current is drawn from the regulator, and consequently the more voltage drop takes place inside the regulator. This causes the terminal voltage (charging voltage) to decrease [37]. The diode V_F measured at a peak of 0.2V under the $1\text{ k}\Omega$ load which indicates that the diode is active and will stop the discharging of a battery if the supply drops to 0V.

Load ($\text{k}\Omega$)	Charging Voltage (V)
0	7.41
1	7.15
10	7.24

Table 4.1: Measured Charging Voltage of the Charging Circuit

High-side Switch on Supply Side

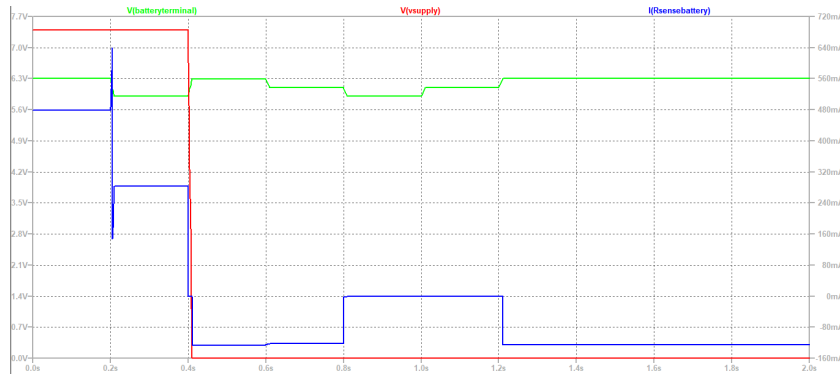
The successful operation of the switch was confirmed through measured voltages as seen below in Table 4.2. For a control signal of 0V, both the V_{GS} of the NMOS and the V_{SG} of the PMOS were measured to be 0V, which indicates that neither the NMOS nor the PMOS were on and so the switch is open. For a control signal of 5V, the V_{GS} of the NMOS was 5.05V and so the NMOS is confirmed to be on. The V_{SG} of the PMOS was 7.43V and so the PMOS is also confirmed to be on which indicates that the switch is closed.

Control Signal (V)	V_{GS} (V)	V_{SG} (V)
0	0	0
5	5.05	7.43

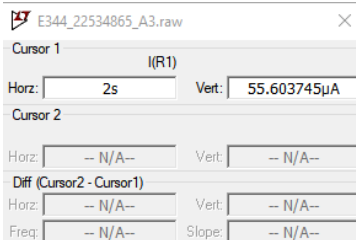
Table 4.2: Measured Switch Terminal Voltages

Under-voltage Protection

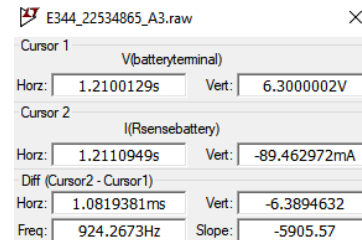
As seen below in Figure 4.2b, the 5V rail will only draw 0.056 mA of current which is below the required 10mA. From Figure 4.2c, the PMOS will also switch between an On/Off state within 1.082 ms of a voltage threshold being reached. Looking at Figure 4.2, it can be seen that initially, the battery will charge because the charging circuit is on. When the charging circuit goes off, any battery voltage above 6V will allow the battery to discharge. After the battery terminals drop below 6V, the battery will stop discharging. This state is switched to at approximately 6V. After this low voltage stage has been reached, the battery will start to discharge again after rising to approximately 6.2V.



(a) Simulation Battery Voltage and Current, Supply Voltage



(b) Simulation 5V Rail Current



(c) Simulation Switching times

Figure 4.2: Simulation Output and Values

The current draw of the 5V rail was measured to be 0.14 mA, which is seen in Figure B.6 and is below the required current draw of 10mA. For the measured results, a $10\text{ k}\Omega$ resistor simulated the battery load. The same behaviour as the simulated results was observed, where the battery would discharge above 6.2V, stop discharging below 6V and then start discharging again at 6.2V. The state of the battery current remained constant during the hysteresis dead-band (as it was designed to do). The exact switching voltages of the battery is observed in Table 4.3.

Discharge Cutoff (V)	Discharge Resumption (V)
6.05V	6.23V

Table 4.3: Measured Discharge Threshold Voltages

Current Sense

For the simulation results, as seen below in Figure 5.1, V_{REF} is observed as 1.75V when no current is flowing through the circuit. When 150mA is discharged from the battery, a $V_{OUT} = 1V$ is observed after a delay of 0.675s. Finally, a $V_{OUT} = 4V$ is observed when 450mA of current charges the battery. For $1mV_{pk}$ noise on R_{SENSE} , $V_{OUT(noise)} = 0.825mV_{pk}$. Similarly, for $49.08mV_{pk}$ noise on V_{REF} (which is attached to the 5V rail), $V_{OUT(noise)} = 0.883mV_{pk}$.

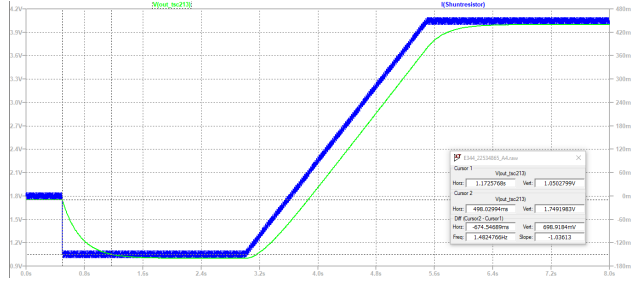
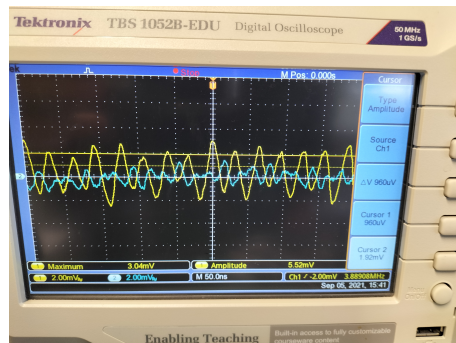


Figure 4.3: TSC213 Output Voltage vs Current through R_{SENSE}

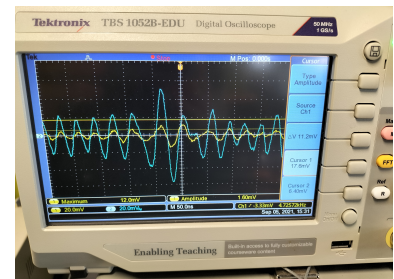
For the measured V_{OUT} , refer to Table 4.4. The results were measured for $V_{BAT} = 6.25V$ and they correspond to the simulation results for the respective voltage vs current values. The noise suppression was also measured as seen in Figure 4.4. For both the noise on the 5V rail and R_{SENSE} , the peak noise of V_{OUT} is less than or equal to double the peak noise of the 5V rail or R_{SENSE} . This confirms that the noise suppression is sufficient if the noise requirements are extrapolated for peak noise levels other than $1mV_{pk}$.

Current System Status	V_{OUT} (V)	I_{SENSE} (mA)
None	1.74	0
Charging	2.77	204
Discharging (3 LEDs)	1.52	46
Discharging (5 LEDs)	1.38	74

Table 4.4: Measured TSC213 Output Voltages and I_{SENSE} Current



(a) 5V Rail Noise (Blue) Vs V_{OUT} Noise (Yellow)



(b) I_{SENSE} Noise (Blue) Vs V_{OUT} Noise (Yellow)

Figure 4.4: Measured Noise Suppression Results

Low-side Switch

The low-side switch was verified successfully by measured voltages and drain currents observed below in Table 4.5. For a control signal of 0V, the V_{GS} of the NMOS was measured to be 0V, which indicates that the NMOS is off and the switch is open thus not allowing current to flow into the load. For a control signal of 5V, the V_{GS} of the NMOS was 5.02V and so the NMOS is confirmed to be on thus closing the switch and allowing current to flow through the load.

Control Signal (V)	V_{GS} (V)	I_D (mA)
0	0	0
5 (3 LEDs)	5.02	46
5 (5 LEDs)	5.02	74

Table 4.5: Measured Switch Terminal Voltages and Drain Currents

Supply Voltage Measurement

The simulated as well as measured results are seen below in Figure 4.5 and Table 4.6. At 0.65s, the circuit output changes to 0.225V when the supply voltage rises to 1V. Following this result, the circuit output rises to 5V when the supply voltage rises to 22V. This indicates that the circuit is responding appropriately to a change in the input voltage. The measured results also indicate an appropriate response to input voltages, although resistor tolerances cause some deviations from ideal behaviour. When a 1V step change is applied, the circuit output responds appropriately within 19.6ms, as seen in Figure 4.6. The noise on the output is within the specification limits.

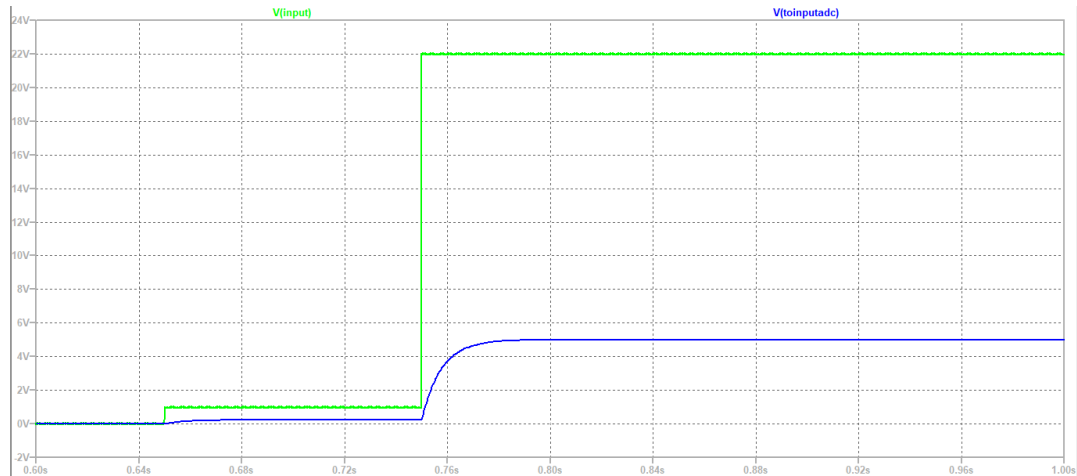


Figure 4.5: Simulated Supply Voltages vs Circuit Output Voltages

Supply Voltage (V)	Measured Output Voltage (V)
0.0	0.000
5.5	1.264
11.0	2.860
16.5	3.792
22.0	5.057

Table 4.6: Measured Supply Voltage vs Measured Output Voltage

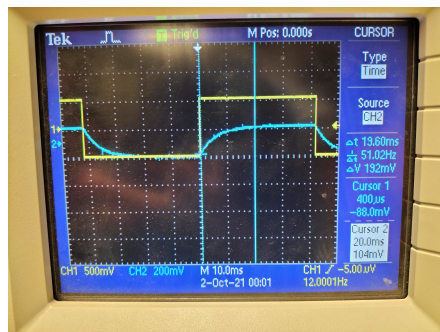


Figure 4.6: Supply Voltage Measurement Circuit Response Time

Battery Voltage Measurement

The simulated results are seen below in Figure 4.7. At 0.1s, the circuit output changes from 0.57V to 2.97V when the battery voltage changes from 5.7 to 6.7V. Following this, at 0.25s, the circuit output increases from 2.97V to 4.89V when the battery voltage increases from 6.7V to 7.5V. Finally, the circuit output drops from 4.89V to 0.57V when the battery voltage drops from 7.5V to 5.7V. It can then be seen that the battery voltage measurement circuit performs accurately (covers the range designed for) and has a response time within specification limits.



Figure 4.7: Simulated Battery Voltages vs Circuit Output Voltages

For the measured results, the measured output voltages are consistent with the simulated results at the same battery voltages. The full range of V_{OUT} is 0.237V to 4.9V. The bottom of the range is above what was designed for due to resistor tolerances. The circuit responds to an input change within $10.8\mu s$, which is within the specification limits.

Battery Voltage (V)	Measured Output Voltage (V)
5.5	0.237
6.0	1.432
6.6	2.860
7.2	4.370
7.5	4.900

Table 4.7: Measured Battery Voltage vs Measured Output Voltage

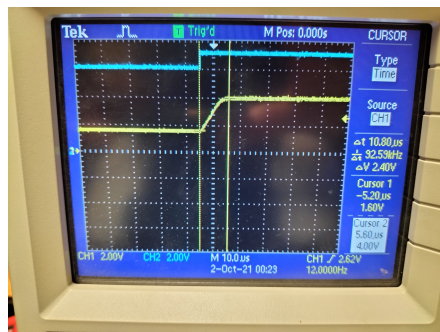


Figure 4.8: Battery Voltage Measurement Circuit Response Time

Chapter 5

System Results

The charging circuit in combination with the high side switch is able to charge the battery to the designed voltage with an appropriate current limit. This battery is also able to supply current to the load without depleting to harmful levels. All of these operations are also correctly monitored by the current sensing circuit which will later be used as input to a micro-controller.

It can then be observed from the design and results of each modular part of the overall circuit, that the complete system functions according to the requirements. Safety measures in the form of a fuse have also been implemented to minimise fatal mistakes in the operation of the system.

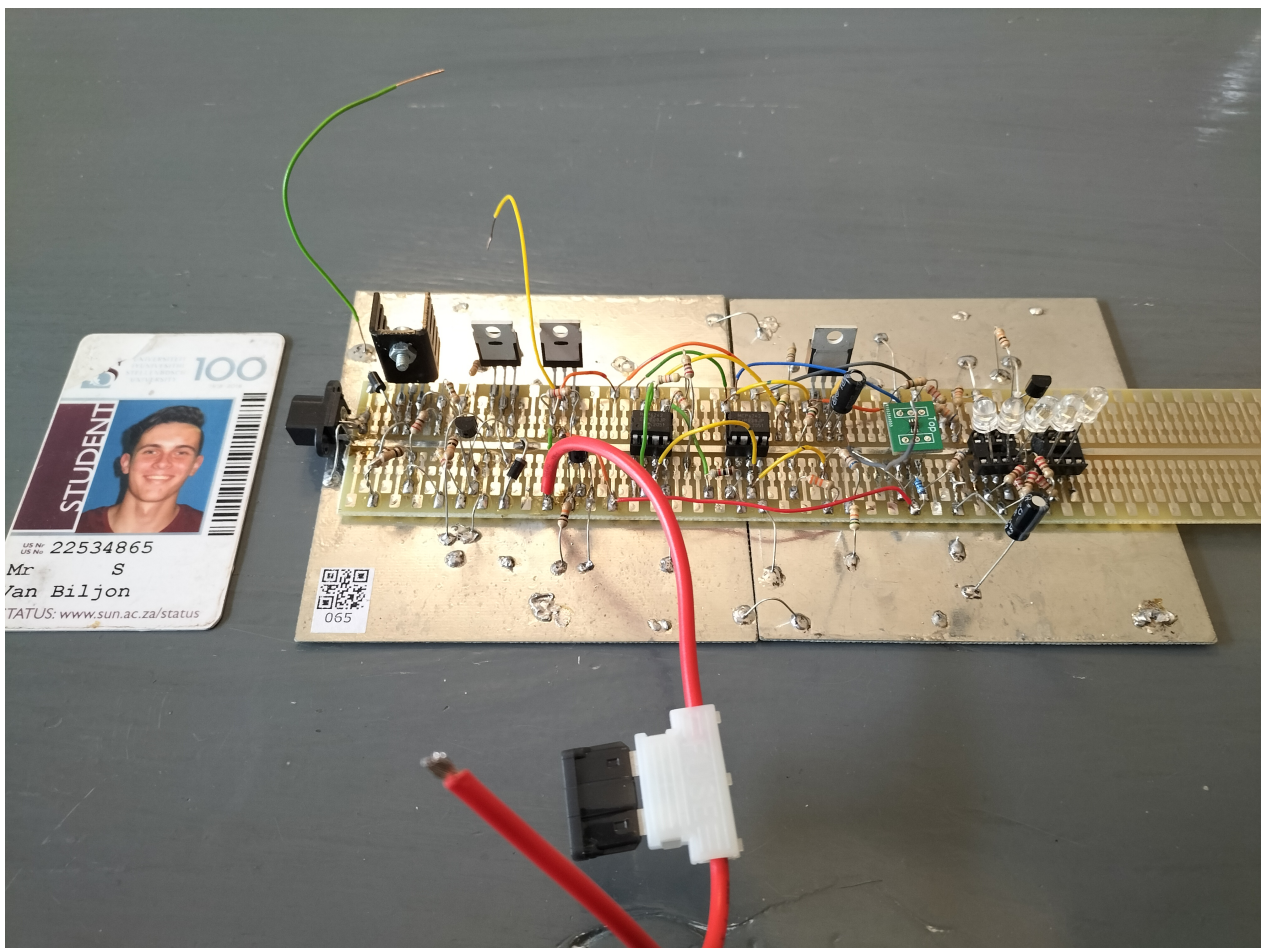


Figure 5.1: PCB with barcode and student card

Bibliography

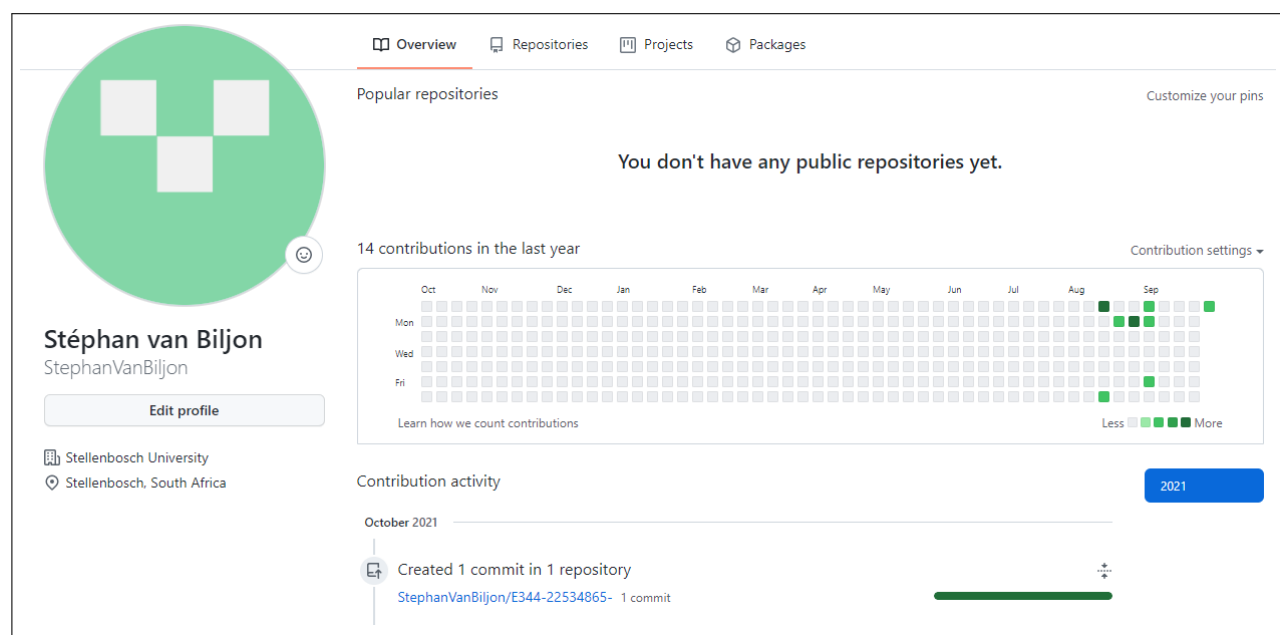
- [1] Christiana Honsberg and Stuart Bowden, “Solar cell parameters: Iv curve.” [Online]. Available: <https://www.pveducation.org/pvcdrom/solar-cell-operation/iv-curve>
- [2] Electronic Products, “Higher power comes to solar technology,” 2011. [Online]. Available: <https://www.electronicproducts.com/higher-power-comes-to-solar-technology/>
- [3] James Lewis, “Low side vs. high side transistor switch,” 2019. [Online]. Available: <https://www.baldengineer.com/low-side-vs-high-side-transistor-switch.html>
- [4] ElectronicsBeliever, “High side driver design using pmos with resistive load,” 2015. [Online]. Available: <http://electronicsbeliever.com/high-side-driver-design-using-pmos-with-resistive-load/>
- [5] Buzai Andras, “P-channel mosfet high side switch,” 2012. [Online]. Available: <https://electronics.stackexchange.com/questions/42030/p-channel-mosfet-high-side-switch>
- [6] CHARGETEK, “Battery charger basics.” [Online]. Available: <https://chargetek.com/basic-information.html>
- [7] RS Pro, “Sealed lead-acid battery 537-5422(6v4.0ah) general purpose specification.” [Online]. Available: https://learn.sun.ac.za/pluginfile.php/2876542/mod_resource/content/0/battery.pdf
- [8] Electronics Tutorials, “Inverting schmitt trigger.” [Online]. Available: <https://www.electronics-tutorial.net/analog-integrated-circuits/schmitt-trigger/inverting-schmitt-trigger/>
- [9] planete energies, “How does a photovoltaic cell work?” 2019. [Online]. Available: <https://www.planete-energies.com/en/medias/close/how-does-photovoltaic-cell-work>
- [10] GEOTHERM, “Polycrystalline solar cells vs monocrystalline: Which is better?” [Online]. Available: <https://geothermhvac.com/mono-vs-poly-better/>
- [11] Christiana Honsberg and Stuart Bowden, “Solar cell parameters: Open-circuit voltage.” [Online]. Available: <https://www.pveducation.org/pvcdrom/solar-cell-operation/open-circuit-voltage>
- [12] ——, “Solar cell parameters: Short-circuit current.” [Online]. Available: <https://www.pveducation.org/pvcdrom/solar-cell-operation/short-circuit-current>

- [13] ACDC Dynamics, “Slp005-12 pv module product specification sheet.” [Online]. Available: [https://learn.sun.ac.za/pluginfile.php/2893563/mod_resource/content/0/SLP005-12\\$%\\$20PV\\$%\\$20Module.pdf](https://learn.sun.ac.za/pluginfile.php/2893563/mod_resource/content/0/SLP005-12$%$20PV$%$20Module.pdf)
- [14] Explore UL, “Standard test conditions.” [Online]. Available: https://www.homerenergy.com/products/pro/docs/latest/standard_test_conditions.html
- [15] Christiana Honsberg and Stuart Bowden, “Lead acid batteries.” [Online]. Available: <https://www.pveducation.org/pvcdrom/batteries/lead-acid-batteries>
- [16] intercel, “Temperature effects on batteries.” [Online]. Available: <https://www.intercel.eu/frequently-asked-questions/temperature-effects-on-batteries/>
- [17] Booysen, MJ, “Video: Assignment 1 overview,” 2021. [Online]. Available: <https://learn.sun.ac.za/mod/resource/view.php?id=1541290>
- [18] BYJU’S, “Internal resistance formula.” [Online]. Available: [https://byjus.com/internal-resistance-formula/#:~:text=Internal%\\$%20resistance%\\$%20refers%\\$%20to%\\$%20the,%\\$%3D%\\$%20I%\\$%20\(r%\\$%20%\\$%2B%\\$%20R\)](https://byjus.com/internal-resistance-formula/#:~:text=Internal%$%20resistance%$%20refers%$%20to%$%20the,%$%3D%$%20I%$%20(r%$%20%$%2B%$%20R))
- [19] Shawn Hymel, “Measuring internal resistance of batteries.” [Online]. Available: <https://learn.sparkfun.com/tutorials/measuring-internal-resistance-of-batteries/internal-resistance>
- [20] Littelfuse, “Fuseology.” [Online]. Available: https://www.littelfuse.com/~/media/automotive/catalogs/littelfuse_fuseology.pdf
- [21] ArcFlash, “Stability of fuses over time,” 2017. [Online]. Available: <https://brainfiller.com/arcflashforum/viewtopic.php?f=2&t=4309>
- [22] STMicroelectronics, “Lm217, lm317 - 1.2 v to 37 v adjustable voltage regulators,” 2014. [Online]. Available: https://learn.sun.ac.za/pluginfile.php/2893561/mod_resource/content/0/LM317T.pdf
- [23] HY, “1n5817 thru 1n5819 datasheet,” 2014. [Online]. Available: https://learn.sun.ac.za/pluginfile.php/2893560/mod_resource/content/0/1N5819.pdf
- [24] Internatonal Rectifier, “Irf9z24npbf product specification sheet.” [Online]. Available: https://learn.sun.ac.za/pluginfile.php/2876541/mod_resource/content/0/IRF9Z24NPBF.pdf
- [25] AAVID THERMALOY, “To-220 heat sinks.” [Online]. Available: [https://learn.sun.ac.za/pluginfile.php/2893566/mod_resource/content/0/TO-220%\\$%20Heat%\\$%20Sinks.pdf](https://learn.sun.ac.za/pluginfile.php/2893566/mod_resource/content/0/TO-220%$%20Heat%$%20Sinks.pdf)
- [26] STMicroelectronics, “Tip41c product specification sheet.” [Online]. Available: <https://www.alldatasheet.com/view.jsp?Searchword=Tip41c&gclid=CjwKCAjw64eJBhAGEiwABr9o2JOOctvaIvN9nV4Gahsm3a70jbeHWUC1wOuO49TGK1E6HAeTiTTBwE>

- [27] Luke James / Erika Granath, “What’s the difference between mosfet and bjt?” 2020. [Online]. Available: <https://www.power-and-beyond.com/whats-the-difference-between-mosfet-and-bjt-a-909006/>
- [28] Electronics Tutorials, “The schottky diode,” 2019. [Online]. Available: <https://www.electronics-tutorials.ws/diode/schottky-diode.html>
- [29] ON Semiconductor, “2n7000 / 2n7002 / nds7002a n-channel enhancement mode field effect transistor.” [Online]. Available: https://learn.sun.ac.za/pluginfile.php/2876543/mod_resource/content/0/2N7000.pdf
- [30] CREE, “Cree 5-mm round led c503d-wan.” [Online]. Available: https://learn.sun.ac.za/pluginfile.php/2893565/mod_resource/content/0/Cree%205%20mm%20Round%20LED%20-%20Cool%20White.pdf
- [31] RSPRO, “Rs pro 5a tan automotive blade fuse.” [Online]. Available: https://learn.sun.ac.za/pluginfile.php/2893574/mod_resource/content/0/RSPro_Fuses.pdf
- [32] Texas Instruments, “Lm2940x 1-a low dropout regulator.” [Online]. Available: https://learn.sun.ac.za/pluginfile.php/2876545/mod_resource/content/0/LM2940.pdf
- [33] ——, “A7800 series positive-voltage regulators.” [Online]. Available: https://learn.sun.ac.za/pluginfile.php/2893559/mod_resource/content/0/LM7805.pdf
- [34] Microchip, “50 μ a, 550 khz rail-to-rail op amp,” 2008. [Online]. Available: https://learn.sun.ac.za/pluginfile.php/2893569/mod_resource/content/0/MCP6241.pdf
- [35] STMicroelectronics, “High/low-side, bidirectional, zero-drift current sense amplifiers,” 2020. [Online]. Available: https://learn.sun.ac.za/pluginfile.php/2876544/mod_resource/content/0/TSC213.pdf
- [36] Atmel, “Atmega16u4/atmega32u4,” 2016. [Online]. Available: https://ww1.microchip.com/downloads/en/DeviceDoc/Atmel-7766-8-bit-AVR-ATmega16U4-32U4_Datasheet.pdf
- [37] Electrical Volt, “Why is the terminal voltage less than emf during discharging of battery?” 2020. [Online]. Available: <https://www.electricalvolt.com/2020/08/why-is-the-terminal-voltage-less-than-emf-during-discharging-of-battery/#:~:text=The%20lower%20value%20of%20load,will%20be%20less%20terminal%20voltage.>

Appendix A

GitHub Activity Heatmap



Appendix B

Stuff you want to include

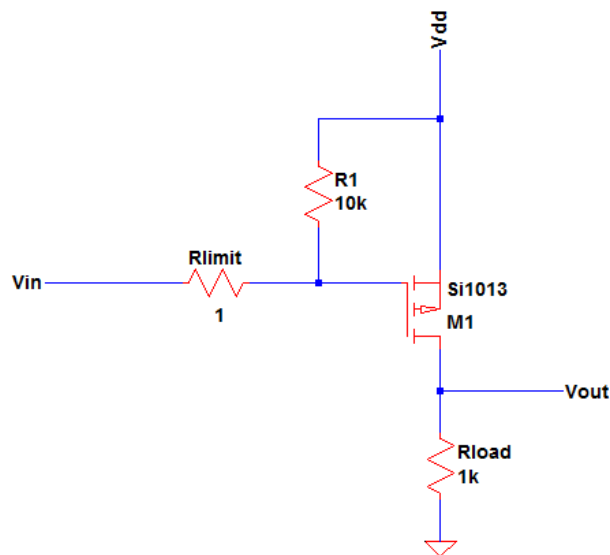


Figure B.1: High-side PMOS switch [4]

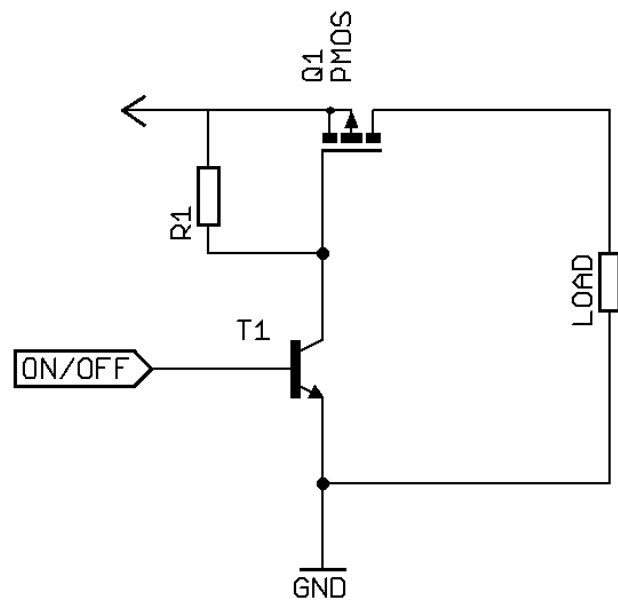


Figure B.2: High-side PMOS switch with NPN driver [5]

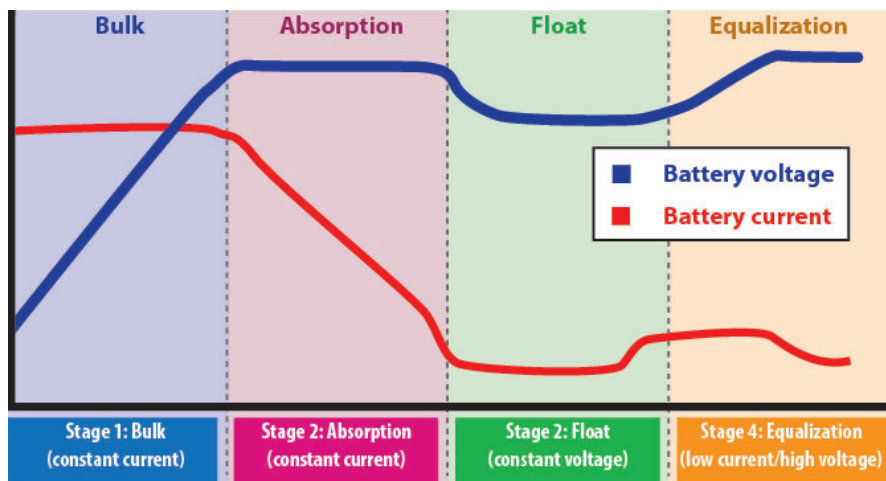


Figure B.3: Charging stages of a battery [6]

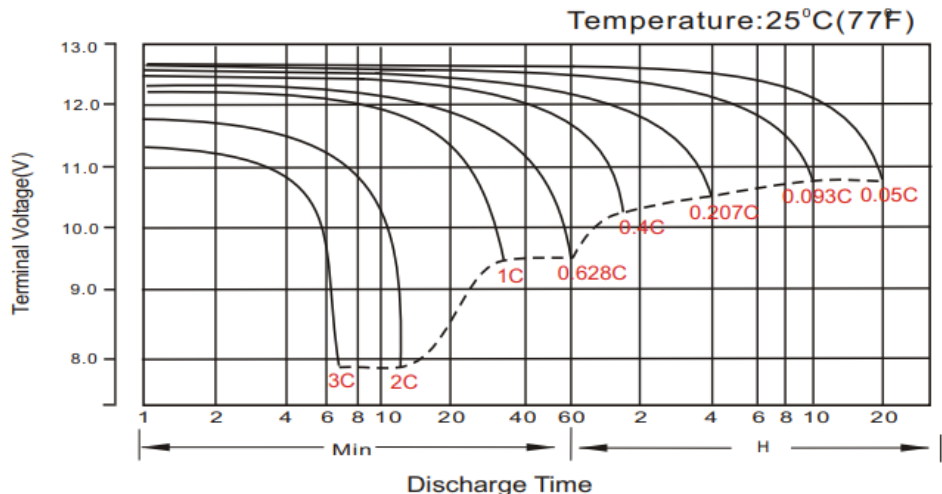


Figure B.4: RS-4AH Discharge Characteristics [7]

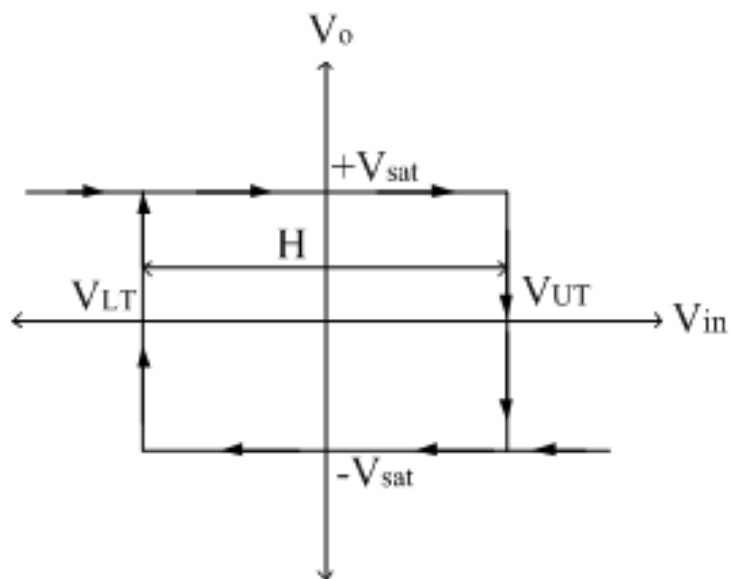


Figure B.5: Hysteresis Curve of an Inverting Schmitt Trigger with $V_{REF} = 0V$ [8]



Figure B.6: Current Draw of the 5V Rail (B) with a Voltage Over the Load (A)